EPJ Web of Conferences **302**, 07004 (2024) https://doi.org/10.1051/epjconf/202430207004
*SNA + MC 2024*

# Compendium on Monte Carlo simulation of photoneutrons in the Giant Dipole Resonance energy range: the first five elements

*Louis* Garnaud[1], *Luna* Sobczak[2], *Johann* Piekar[2], *Adrien* Sari[2*], *Alexis* Jinaphanh[1], *Amine* Nasri[3], *Cédric* Jouanne[1], *Tatsuhiko* Ogawa[4], and *Andrea* Zoia[1]

[1]Université Paris-Saclay, CEA, SERMA, 91191 Gif-sur-Yvette, France
[2]Université Paris-Saclay, CEA, List, 91120 Palaiseau, France
[3]CEA, DAM, DIF, F-91297 Arpajon, France
[4]Japan Atomic Energy Agency, 2-4 Shirakata, Tokai-mura, Naka-gun, Ibaraki 319-1106, Japan

**Abstract.** Neutrons generated by photonuclear reactions, "photoneutrons", are encountered in various applications involving high-energy gamma sources, electron accelerators or nuclear reactors. Monte Carlo particle-transport codes are generally used to simulate the emission of photoneutrons, characterize their field or assess their impact on nuclear systems. The aim of this work is to create a compendium on the simulation of photoneutrons using several Monte Carlo codes, i.e., MCNP6, PHITS and TRIPOLI-4, each code being run successively with ENDF/B-VIII.0 and JENDL-5 nuclear data libraries. We study the photoneutron fields produced by 50 elements with their natural isotopic composition from the reaction energy threshold up to 30 MeV, i.e., in the regime of the Giant Dipole Resonance (GDR). The photoneutron fields are characterized according to three observables, i.e., photoneutron current, energy spectrum and angular distribution. This paper presents the results obtained for the first five elements in order of increasing atomic number, i.e., deuterium, beryllium, carbon, nitrogen and oxygen. The compendium could serve as a handbook for users to master the current strengths and limitations of the codes, for code developers to make progress in the sampling of neutron-emitting photonuclear reactions, and more broadly for all researchers working on photoneutrons, whether they are evaluators of nuclear data libraries or experimental nuclear physicists.

## 1 Introduction

The interaction between a high-energy photon and the nucleus of an atom may induce photonuclear reactions. These events can lead to the expulsion of neutrons, known as "photoneutrons". The Giant Dipole Resonance (GDR) phenomenon, which can be described as an oscillation of all the neutrons against all the protons inside the atomic nucleus, is the main mechanism responsible for the emission of photoneutrons below 30 MeV. Photoneutrons are encountered in various applications involving high-energy gamma

* Corresponding author: adrien.sari@cea.fr

sources, electron accelerators or nuclear reactors. Monte Carlo particle-transport codes are generally used to simulate photoneutrons, characterize their field or assess their impact on nuclear systems [1, 2].

This work aims at creating a compendium on the simulation of photoneutrons using several independently developed Monte Carlo codes, i.e., MCNP6 [3, 4], PHITS [5, 6] and TRIPOLI-4 [7, 8], each code being run successively with ENDF/B-VIII.0 [9] and JENDL-5 [10] nuclear data libraries. We study the photoneutron fields produced by 50 elements with their natural isotopic composition from the reaction energy threshold up to 30 MeV, i.e., in the regime of the Giant Dipole Resonance (GDR). The photoneutron fields are characterized according to three observables, i.e., photoneutron current, energy spectrum and angular distribution.

This paper presents the results obtained for the first five elements in order of increasing atomic number, i.e., deuterium, beryllium, carbon, nitrogen and oxygen. The compendium could serve as a reference database for users to master the current strengths and limitations of the codes, for code developers to make progress in the sampling of neutron-emitting photonuclear reactions, and more broadly for all researchers working on photoneutrons, whether they are evaluators of nuclear data libraries or experimental nuclear physicists.

This work is organized as follows. In section 2, we describe the benchmark method and the Monte Carlo simulation model, and illustrate briefly the Monte Carlo codes and nuclear data libraries used in this study. In section 3, we present and discuss the simulation results, whereas general comments are provided in section 4. Finally, conclusions are drawn in section 5.

## 2 Materials and methods

### 2.1 Benchmark method

We benchmark the following Monte Carlo particle-transport simulation codes:

- MCNP6.3 [3, 4];
- PHITS version 3.34 [5, 6],
- TRIPOLI-4 version 12 [7, 8].

Each code is run twice, with two reference nuclear data libraries, i.e., ENDF/B-VIII.0 [9] and JENDL-5 [10].

Similarly as proposed in a previous investigation [11], we characterize the photoneutron fields according to three observables:

- particle current;
- energy spectrum;
- angular distribution.

### 2.2 Monte Carlo simulation model

For the purpose of this work, we have introduced a simplified benchmark configuration. The target is a 5 mm-diameter sphere irradiated by monoenergetic photons whose energy range extends from the (γ, n) reaction threshold to 30 MeV, by 1 MeV steps. The distance between the photon source and the target is 1 mm, and the target is surrounded by vacuum. Figure 1 illustrates the corresponding Monte Carlo simulation model.

The densities and isotopic compositions of the targets are taken from reference [12]. However, if the density is lower than 1 $g.cm^{-3}$, we set artificially the density at 1 $g.cm^{-3}$ in order to increase the statistics of simulation results. Table 1 gathers the densities and isotopic compositions of the five elements considered in this work.

**Table 1.** The five elements considered in this work: densities and isotopic compositions.

| Element | Density (g.cm$^{-3}$) | Isotope | Atom fraction (%) |
|---|---|---|---|
| Deuterium | 1 | $^{2}$H | 100 |
| Beryllium | 1.85 | $^{9}$Be | 100 |
| Carbon | 2.2 | $^{12}$C | 98.93 |
| | | $^{13}$C | 1.07 |
| Nitrogen | 1 | $^{14}$N | 99.636 |
| | | $^{15}$N | 0.364 |
| Oxygen | 1 | $^{16}$O | 99.962 |
| | | $^{17}$O | 0.038 |

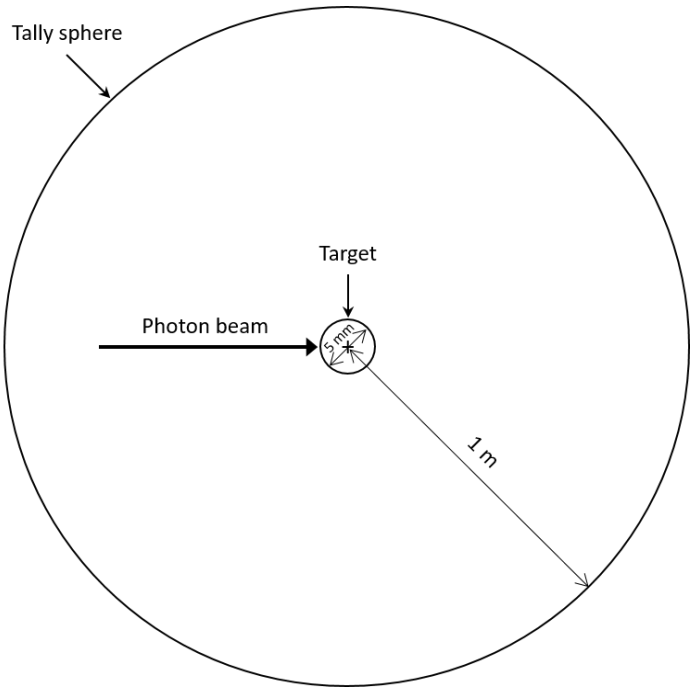


**Fig. 1.** Schematic representation (not to scale) of the simulation model of the 5 mm-diameter spherical target irradiated by monoenergetic photons from the (γ, n) reaction energy threshold to 30 MeV.

As shown in Fig. 1, the simulation model includes a 1 m-radius sphere centred on the target in order to score the three photoneutron tallies, i.e., particle current, energy spectrum and angular distribution. To estimate the photoneutron currents, we used the following tally options:

- *F1* tallies in MCNP6;
- *CURRENT* responses in TRIPOLI-4;
- *[T-Cross]* tallies in PHITS.

The photoneutron energy spectra are determined using 10 keV-energy bins, whereas 4° polar angle bins are used to tally the photoneutron angular distributions, with the 0° reference vector corresponding to the direction of the photon source.

## 2.3 Monte Carlo codes

### *2.3.1 MCNP6*

MCNP6 [3, 4] is a three dimensional continuous-energy Monte Carlo code developed by LANL (New Mexico, USA). MCNP6 is written in Fortran and allows simulating neutrons, photons, electromagnetic shower and up to 37 different particles. For nuclear reactions, MCNP6 uses classical physics kinematics. Nuclear data for MCNP6 are based on the ENDF-6 format and managed by the NJOY nuclear data processing system. For this study, in the *PHYS:P* card (photon physics), the *ispn* option is set to 1 in order to activate photonuclear reactions together with a special variance-reduction option for their sampling. This option forces photonuclear reactions at each photoatomic event and modifies their statistical weights in order to preserve a fair Monte Carlo game.

### *2.3.2 PHITS*

PHITS [5, 6] is a general-purpose Monte Carlo particle-transport code developed under collaboration between JAEA, RIST, KEK and several other institutes (Japan). PHITS is written in Fortran and can simulate almost all kinds of particles, including neutrons, photons and electromagnetic shower over a wide range of energies thanks to nuclear data and nuclear reaction models. For nuclear reactions, PHITS uses relativistic physics kinematics. Nuclear data used in PHITS are in ACE format, based on the ENDF-6 format processed by NJOY, as for MCNP6. Variance reduction is enforced on photonuclear reactions with the parameter *pnimul=100*, which basically alters their natural occurrence rate.

In this study, we used PHITS ver. 3.34. However, since an updated version of the code is currently under development to improve the simulation of photonuclear reactions for light elements, it is planned to run again the PHITS calculations as soon as this new version of the code is released. The updated results will be included in an extended version of this paper.

### *2.3.3 TRIPOLI-4*

TRIPOLI-4 [7, 8] is a three-dimensional continuous-energy Monte Carlo code developed by CEA, Paris-Saclay center, France. TRIPOLI-4 is written in C++ and can simulate neutrons, photons and electromagnetic shower. For nuclear reactions, TRIPOLI-4 uses semi-relativistic physics kinematics. Nuclear data for TRIPOLI-4 are based on the ENDF-6 format and managed by the nuclear data processing system GALILEE. In order to improve the statistics, photonuclear reactions are forced at each photon collision, their statistical weight is modified, and the Russian roulette threshold is correspondingly adjusted on the sampled photoneutrons.

### 2.4 Nuclear data libraries

#### *2.4.1 ENDF/B-VIII.0*

The latest revision of the U.S.'s Evaluated Nuclear Data File (ENDF) library is ENDF/B-VIII.0 [9]. For this work, we use the following sub-libraries in the format accepted by each code:

- EPDL97 [13] for photoatomic reactions, released in 1997;
- ENDF7u [14] for photonuclear reactions, released in 2007;
- ENDF/B-VIII.0 [9] for neutron reactions, released in 2018.

#### *2.4.2 JENDL-5*

The fifth version of Japanese Evaluated Nuclear Data Library (JENDL) – JENDL-5 [10] – was released in 2021. For this work, we have used the JENDL-5 library for the following sub-libraries: photoatomic reactions, photonuclear reactions and neutrons reactions. It should be noted that photoatomic nuclear data in JENDL-5 are taken from ENDF/B-VIII.0.

## 3 Results and discussion

This paper presents the results obtained for the first five elements in the database in ascending order of atomic number, i.e., deuterium, beryllium, carbon, nitrogen and oxygen. The involved computational effort is considerable: this first version of the compendium required 774 runs on different configurations, which represents about three weeks of calculation time on 384 CPUs.

For each material, we present the photoneutron currents as a function of the photon source energy. The photoneutron energy spectra and angular distributions are plotted for the case of 20 MeV photons, and are normalized in order to enable a fair comparison of the shapes of the curves. For each figure of angular distributions, a short-dashed horizontal line represents the ideal isotropic emission line, for reference. For the ease of comparison, when plotting side-by-side two figures, x-axis and y-axis scales have been set to be the same on both sides.

### 3.1 Deuterium

Figures 2, 3 and 4 present respectively the currents, the normalized energy spectra and angular distributions of photoneutrons emitted by the deuterium target irradiated by monoenergetic photons in the 3–30 MeV range, simulated with MCNP6, PHITS and TRIPOLI-4, using ENDF/B-VIII.0 or JENDL-5 nuclear data libraries.

The photoneutron currents show some differences between the two libraries especially for the lowest photon energies, from 3 to 9 MeV, with ENDF/B-VIII.0 below JENDL-5. Between 9 and 25 MeV, the two libraries show a good agreement. However, beyond 25 MeV, ENDF/B-VIII.0 is above JENDL-5. Results from MCNP6 and TRIPOLI-4 are in good agreement, while PHITS results are shifted towards lower values.

The photoneutron energy spectra show a good agreement between TRIPOLI-4 with JENDL-5, TRIPOLI-4 with ENDF/B-VIII.0, and PHITS with JENDL-5. For this nucleus, JENDL-5 and ENDF/B-VIII.0 describe the single (γ, n) reaction as a two-body reaction, which, by using the angular distribution in the centre of mass frame, makes it possible to define without ambiguity the characteristics of the emitted neutron and proton. MCNP6 presents sharp peaks at high-energy, which demonstrates a problem in the treatment of kinematics in the laboratory frame. PHITS with ENDF/B-VIII.0 and MCNP6 with ENDF/B-VIII.0 are shifted around 12 MeV. These results could be explained by an issue in the NJOY version used to process the ENDF data to ACE files for MCNP6. The JENDL-5 ACE files were produced by JAEA with a modified version of NJOY, and seem to match with TRIPOLI-4.

### 3.2 Beryllium

Figures 5, 6 and 7 present respectively the currents, the normalized energy spectra and angular distributions of photoneutrons emitted by the beryllium target irradiated by monoenergetic photons in the 2–20 MeV range, simulated with MCNP6, PHITS and TRIPOLI-4, using ENDF/B-VIII.0 or JENDL-5 nuclear data libraries.

The photoneutron currents are consistent between the codes and the libraries between 11 and 16 MeV. However, above this energy, MCNP6 and TRIPOLI-4 agree with each other, whereas PHITS stands alone. With ENDF/B-VIII.0 and JENDL-5, TRIPOLI-4 and MCNP6 show a good agreement. PHITS underestimates the photoneutron currents with respect to MCNP6 and TRIPOLI-4. Below 11 MeV, the codes present a good agreement for each library. Results obtained above 20 MeV are not presented, as JENDL-5 and ENDF/B-VIII.0 do not provide data for neutron transport above this energy.

For the photoneutron energy spectra, the codes show a good agreement for each library in almost the entire energy range, with all sharp peaks located in the same energy range. The peaks obtained with MCNP6 are a bit wider than for deuterium; however, we can still notice the effect of non-relativistic kinematics in the code. The heavier the element, the weaker the effect. The energies of the peaks differ for the two libraries selected, indicating different kinematics for the fragmentation reactions of $^{9}$Be.

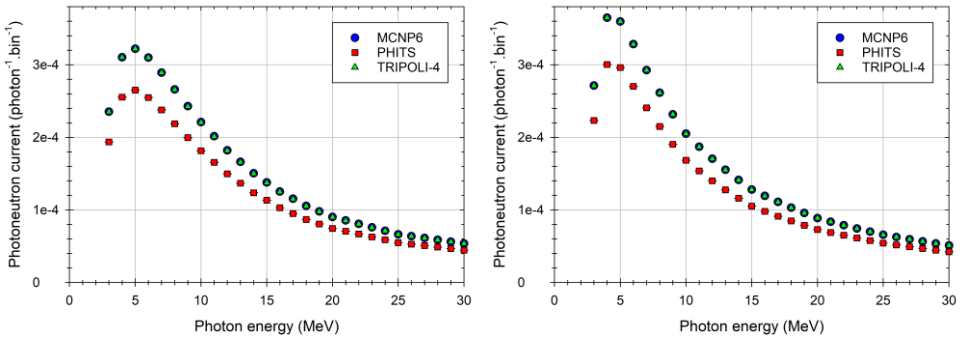


**Fig. 2.** Currents of photoneutrons emitted by the deuterium target irradiated by monoenergetic photons from the (γ, n) reaction energy threshold to 30 MeV, simulated with MCNP6, PHITS and TRIPOLI-4. On the left, with ENDF/B-VIII.0. On the right, with JENDL-5.

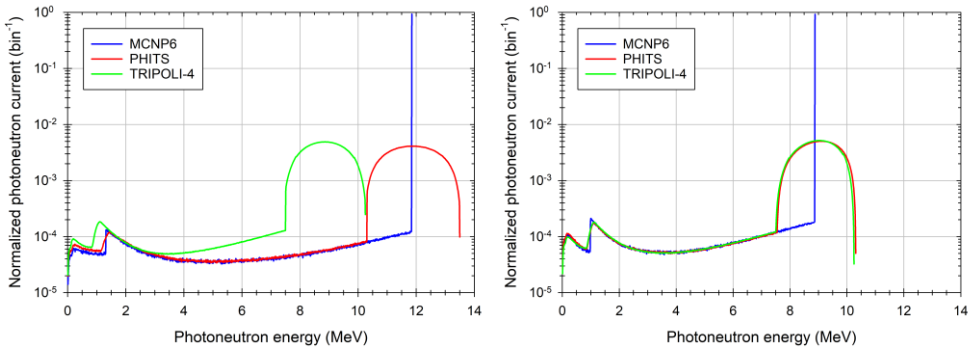


**Fig. 3.** Normalized energy spectra of photoneutrons emitted by the deuterium target irradiated by 20 MeV photons, simulated with MCNP6, PHITS and TRIPOLI-4. On the left, with ENDF/B-VIII.0. On the right, with JENDL-5.

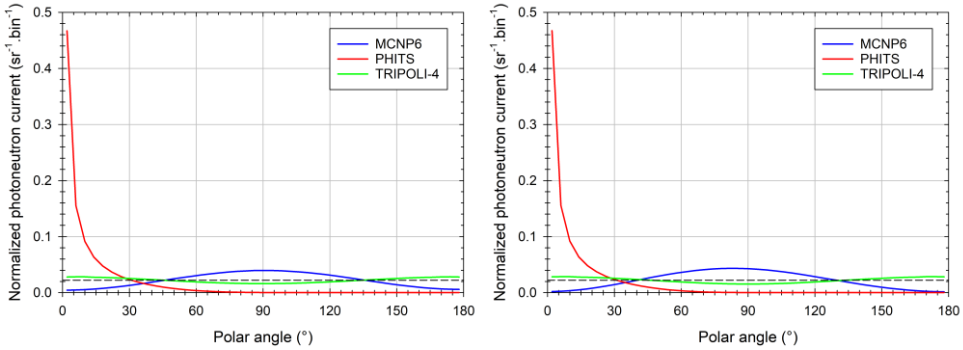


**Fig. 4.** Normalized angular distributions of photoneutrons emitted by the deuterium target irradiated by 20 MeV photons, simulated with MCNP6, PHITS and TRIPOLI-4. On the left, with ENDF/B-VIII.0. On the right, with JENDL-5.

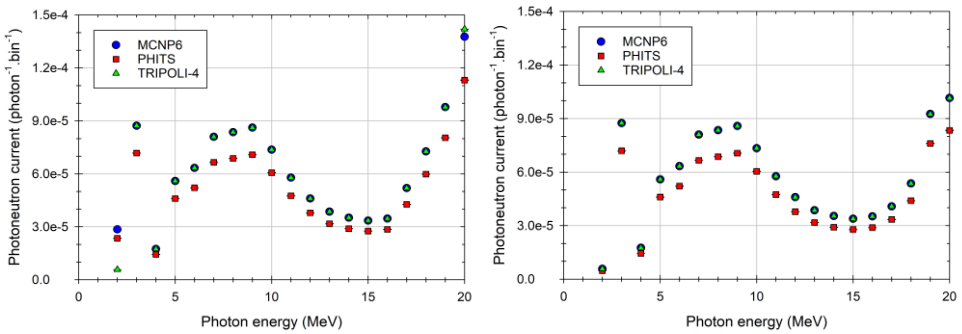


**Fig. 5.** Currents of photoneutrons emitted by the beryllium target irradiated by monoenergetic photons from the (γ, n) reaction energy threshold to 20 MeV, simulated with MCNP6, PHITS and TRIPOLI-4. On the left, with ENDF/B-VIII.0. On the right, with JENDL-5.

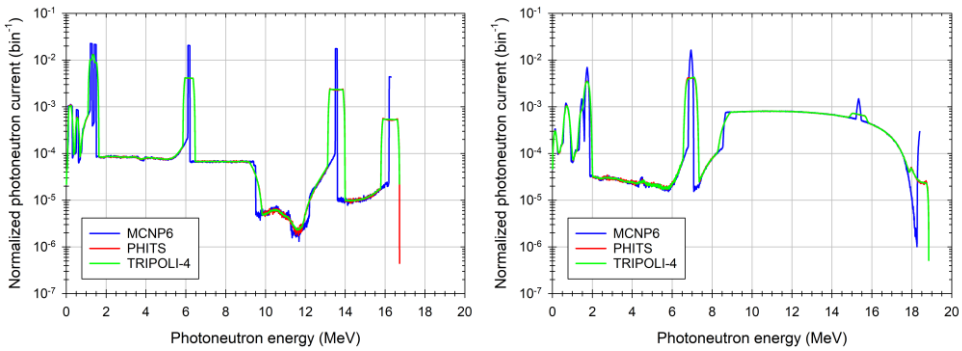


**Fig. 6.** Normalized energy spectra of photoneutrons emitted by the beryllium target irradiated by 20 MeV photons, simulated with MCNP6, PHITS and TRIPOLI-4. On the left, with ENDF/B-VIII.0. On the right, with JENDL-5.

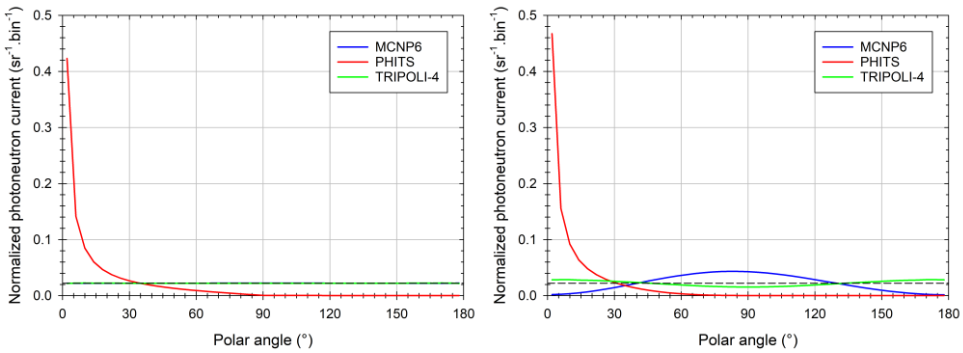


**Fig. 7.** Normalized angular distributions of photoneutrons emitted by the beryllium target irradiated by 20 MeV photons, simulated with MCNP6, PHITS and TRIPOLI-4. On the left, with ENDF/B-VIII.0. On the right, with JENDL-5.

### 3.3 Carbon

Figures 8, 9 and 10 present respectively the currents, the normalized energy spectra and angular distributions of photoneutrons emitted by the carbon target irradiated by monoenergetic photons in the 5–30 MeV range, simulated with MCNP6, PHITS and TRIPOLI-4, using ENDF/B-VIII.0 or JENDL-5 nuclear data libraries.

The photoneutron currents show the same shape, although ENDF/B-VIII.0 overestimates the number of neutrons produced compared to JENDL-5. Only MCNP6 and TRIPOLI-4 show a good agreement with both libraries.

Regarding the photoneutron energy spectrum, all codes are in good agreement. Remark however that each peak is shifted in energy between JENDL-5 and ENDF/B-VIII.0. The first peak around 1 MeV comes from the (γ, n) reaction with $^{12}C$. All other peaks come from reactions with $^{13}C$ and are in most cases related to the excited states of the nucleus. We observe that JENDL-5 yields a larger number of peaks than ENDF/B-VIII.0 probably corresponding to the excited states of the nucleus.

### 3.4 Nitrogen

Figures 11, 12 and 13 present respectively the currents, the normalized energy spectra and angular distributions of photoneutrons emitted by the nitrogen target irradiated by monoenergetic photons in the 11–30 MeV range, simulated with MCNP6, PHITS and TRIPOLI-4, using ENDF/B-VIII.0 or JENDL-5 nuclear data libraries.

For the photoneutron currents, TRIPOLI-4 and MCNP6 show a very good agreement for each library. Moreover, for the two libraries, PHITS slightly underestimates with respect to TRIPOLI-4 and MCNP6.

Regarding the photoneutron energy spectra, at higher energies the shapes are the qualitatively same for the three codes, although the curves are shifted. Once again, at lower energies, JENDL-5 yields a larger number of peaks present in the photoneutron energy spectrum than ENDF/B-VIII.0, which mirrors a more detailed treatment of the excited states of the nucleus.

### 3.5 Oxygen

Figures 14, 15 and 16 present respectively the currents, the normalized energy spectra and angular distributions of photoneutrons emitted by the oxygen target irradiated by monoenergetic photons in the 5–30 MeV range, simulated with MCNP6, PHITS and TRIPOLI-4, using ENDF/B-VIII.0 or JENDL-5 nuclear data libraries. In this material, only $^{16}O$ and $^{17}O$ are simulated.

For the photoneutron currents, with ENDF/B-VIII.0, MCNP6 and TRIPOLI-4 present a good agreement. In addition, observe that oxygen is the only material for which PHITS yields results that lie above MCNP6 and TRIPOLI-4.

Concerning the photoneutron energy spectra, the shapes are qualitatively the same for the three codes, although the curves are once again shifted. The 4 MeV peak is due to the presence of $^{16}O$.

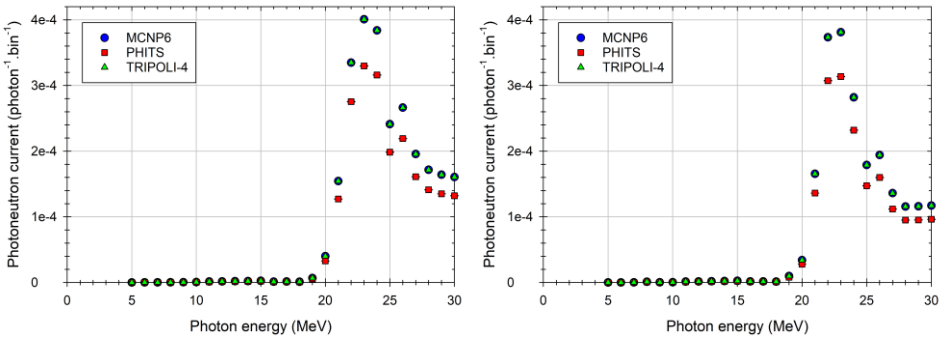


**Fig. 8.** Currents of photoneutrons emitted by the carbon target irradiated by monoenergetic photons from the (γ, n) reaction energy threshold to 30 MeV, simulated with MCNP6, PHITS and TRIPOLI-4. On the left, with ENDF/B-VIII.0. On the right, with JENDL-5.

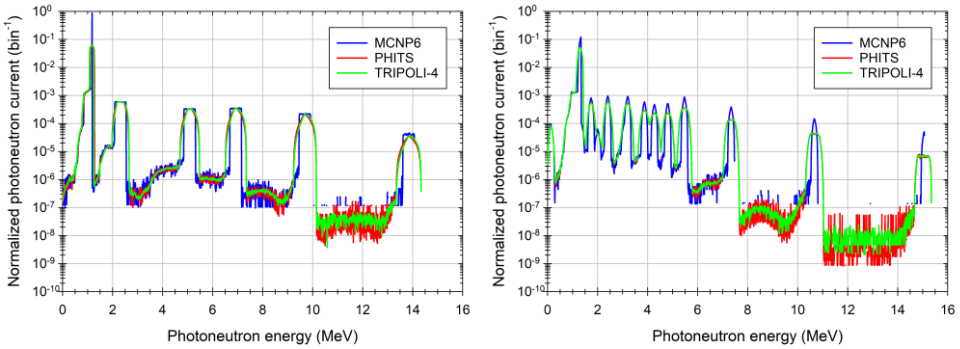


**Fig. 9.** Normalized energy spectra of photoneutrons emitted by the carbon target irradiated by 20 MeV photons, simulated with MCNP6, PHITS and TRIPOLI-4. On the left, with ENDF/B-VIII.0. On the right, with JENDL-5.

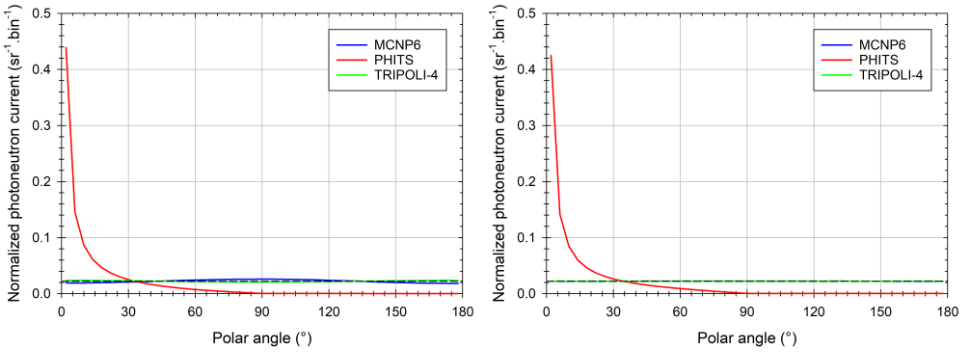


**Fig. 10.** Normalized angular distributions of photoneutrons emitted by the carbon target irradiated by 20 MeV photons, simulated with MCNP6, PHITS and TRIPOLI-4. On the left, with ENDF/B-VIII.0. On the right, with JENDL-5.

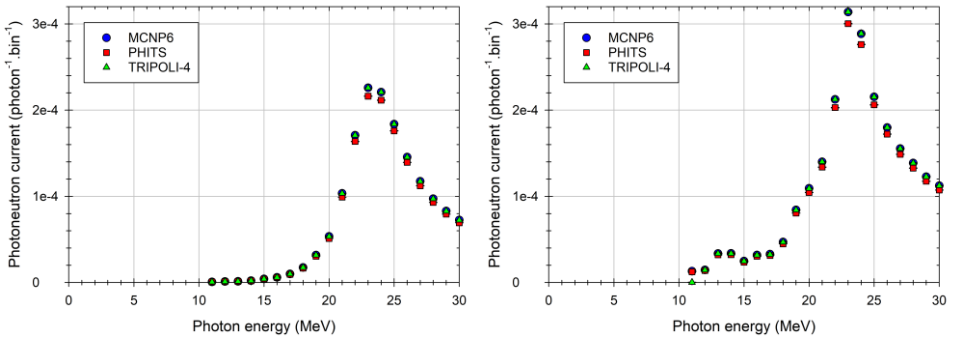


**Fig. 11.** Currents of photoneutrons emitted by the nitrogen target irradiated by monoenergetic photons from the (γ, n) reaction energy threshold to 30 MeV, simulated with MCNP6, PHITS and TRIPOLI-4. On the left, with ENDF/B-VIII.0. On the right, with JENDL-5.

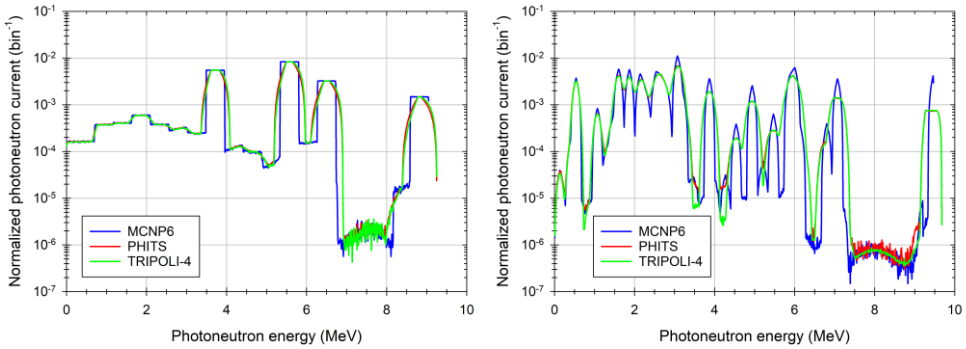


**Fig. 12.** Normalized energy spectra of photoneutrons emitted by the nitrogen target irradiated by 20 MeV photons, simulated with MCNP6, PHITS and TRIPOLI-4. On the left, with ENDF/B-VIII.0. On the right, with JENDL-5.

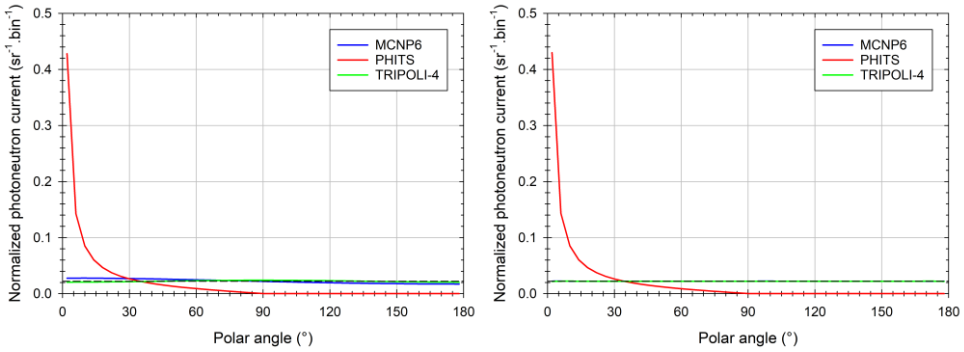


**Fig. 13.** Normalized angular distributions of photoneutrons emitted by the nitrogen target irradiated by 20 MeV photons, simulated with MCNP6, PHITS and TRIPOLI-4. On the left, with ENDF/B-VIII.0. On the right, with JENDL-5.

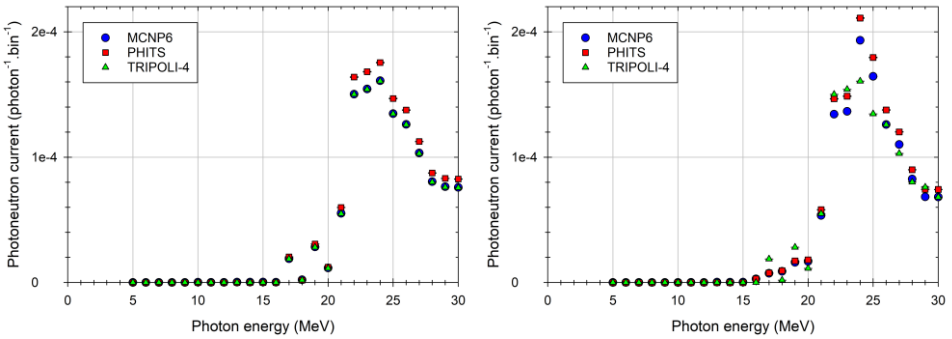


**Fig. 14.** Currents of photoneutrons emitted by the oxygen target irradiated by monoenergetic photons from the (γ, n) reaction energy threshold to 30 MeV, simulated with MCNP6, PHITS and TRIPOLI-4. On the left, with ENDF/B-VIII.0. On the right, with JENDL-5.

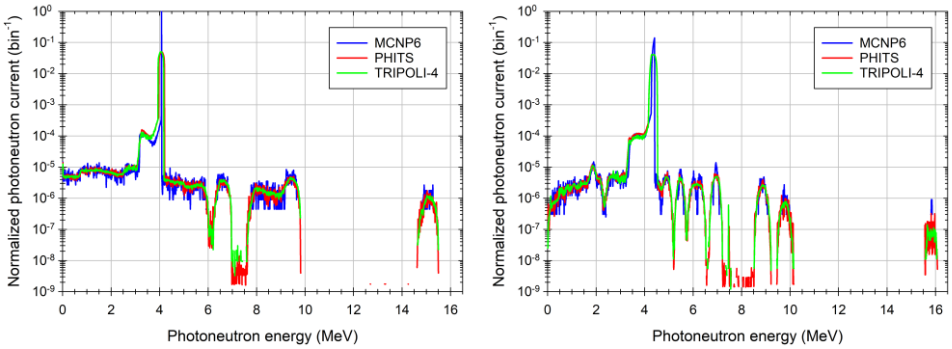


**Fig. 15.** Normalized energy spectra of photoneutrons emitted by the oxygen target irradiated by 20 MeV photons, simulated with MCNP6, PHITS and TRIPOLI-4. On the left, with ENDF/B-VIII.0. On the right, with JENDL-5.

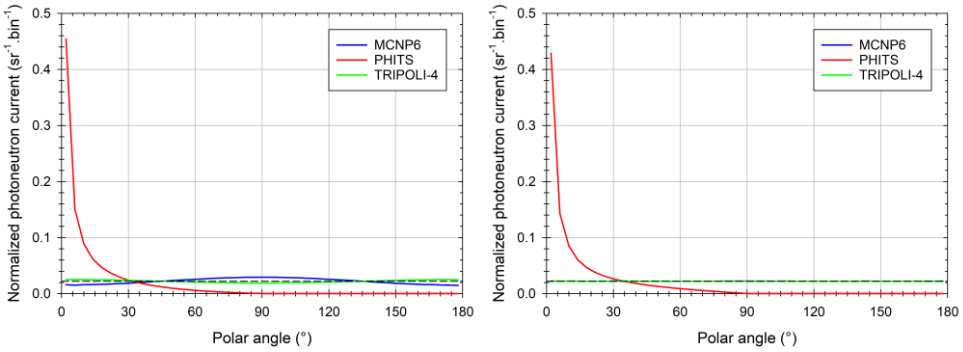


**Fig. 16.** Normalized angular distributions of photoneutrons emitted by the oxygen target irradiated by 20 MeV photons, simulated with MCNP6, PHITS and TRIPOLI-4. On the left, with ENDF/B-VIII.0. On the right, with JENDL-5.

## 4 General comments

In most cases, the integrated photoneutron currents obtained with PHITS are below the ones obtained with MCNP6 and TRIPOLI-4, the two latter codes being most of the time in very good agreement. This observation is still under investigation.

For carbon, nitrogen and oxygen, the photoneutron energy spectra obtained with ENDF/B-VIII.0 and JENDL-5 show a qualitatively similar shape, although shifted in energy by about a few hundreds of keV, which calls for a better understanding of the sampling routines. It should also be noted that TRIPOLI-4 and PHITS exhibit an excellent agreement when comparing these energy spectra, while MCNP6 exhibits a different behaviour in each "peak" of the spectra. Based on this observation, it would be interesting to study the physical kinematics of each reaction in the classical and relativistic formalisms in order to determine the analytical values of each peak energy. For most of the elements, there are several peaks in the spectra, corresponding to the different excited states of the nucleus: in all tested elements, JENDL-5 has a richer structure than ENDF/B-VIII.0 for these excited states, leading to a larger number of peaks. For the extended version of the compendium, we envisage to study in-depth the kinematics of the (γ, n) photonuclear reaction.

Unlike the other codes, PHITS yields photoneutron angular distributions that are markedly anisotropic. The PHITS development team is currently working on this issue encountered with ver. 3.34, which will be corrected in a next version of the code. Once that this new version is released, we will update the results obtained with PHITS and present them in an extended version of the paper. It is also worth noting that for the case of deuterium, beryllium, carbon and oxygen, angular distribution of photoneutrons obtained with MCNP6 and TRIPOLI-4 are in phase opposition. This difference may be due to the non-relativistic treatment of particles in MCNP6.

## 5 Conclusions

The compendium discussed in this paper can be used as a handbook on the Monte Carlo simulation of photoneutrons in the Giant Dipole Resonance (GDR) energy range, and support code users and developers, as well as evaluators of nuclear data libraries and experimental nuclear physicists.

In this work, we have presented the simulation results obtained for the first five elements, in order of increasing atomic number, i.e., deuterium, beryllium, carbon, nitrogen and oxygen. In a forthcoming paper, we will cover an extensive number of elements.

Data will be made available on request.

TRIPOLI-4® is a registered trademark of CEA. The authors thank EDF, Électricité de France, for partial financial support.

## References

1. A. Sari, Appl. Radiat. Isot **191**, 110506 (2023), DOI: 10.1016/j.apradiso.2022.110506
2. K.T. Tran, et al., Nucl. Sci. Eng. **198** (2), 319-335 (2023), DOI: 10.1080/00295639.2023.2195925
3. J.A. Kulesza, et al., MCNP® Code Version 6.3.0 Theory & User Manual, Los Alamos National Laboratory, LA-UR-22-30006, Rev. 1, Los Alamos, NM, USA, 2022, DOI: 10.2172/1889957
4. M.E. Rising, et al., MCNP® Code Version 6.3.0 Release Notes, Los Alamos National Laboratory, LA-UR-22-33103, Rev. 1, Los Alamos, NM, USA, 2023, DOI: 10.2172/1909545
5. T. Sato, et al., J. Nucl. Sci. Technol. **55** (6), 684-690 (2018), DOI: 10.1080/00223131.2017.1419890
6. Y. Iwamoto, et al., J. Nucl. Sci. Technol. **59** (5), 665-675 (2022), DOI: 10.1080/00223131.2021.1993372
7. O. Petit, et al., Prog. Nucl. Sci. Technol. **2**, 798-802 (2011), URL: https://www.aesj.net/document/pnst002/798-802.pdf
8. E. Brun, et al., Ann. Nucl. Energy **82**, 151-160 (2015), DOI: 10.1016/j.anucene.2014.07.053
9. D. Brown, et al., Nucl. Data Sheets **148** (12), 1-142 (2018), DOI: 10.1016/j.nds.2018.02.001
10. O. Iwamoto, et al., J. Nucl. Sci. Technol. **60** (1), 1-60 (2023), DOI: 10.1080/00223131.2022.2141903
11. A. Sari, Nucl. Instrum. Methods Phys. Res. A (to be published)
12. J.R. Rumble, ed., CRC Handbook of Chemistry and Physics, 104th Edition (Internet Version 2023), CRC Press/Taylor & Francis, Boca Raton, FL.
13. D.E. Cullen, J.H. Hubbell, L. Kissel, EPDL97: The Evaluated Photon Data Library '97 Version Lawrence Livermore National Laboratory, UCRL-LR-50400, Vol. 6, Rev. 5, Livermore, CA, USA, 1997, https://digital.library.unt.edu/ark:/67531/metadc678366/m2/1/high_res_d/295438.pdf
14. M.B. Chadwick, et al., Nucl. Data Sheets **112** (12), 2887-2996 (2011), DOI: 10.1016/j.nds.2011.11.002